Inter-decadal changes in intensity of the Oxygen Minimum Zone off Concepción, Chile (~36°S) over the last century

Benjamín Srain[1], Silvio Pantoja[2, 3], Julio Sepúlveda[4,*], Carina Lange[2,3], Praxedes Muñoz[5], Roger E. Summons[4], Jennifer McKay[6], Marco Salamanca[2]

[1] {Graduate Program in Oceanography, Department of Oceanography, University of Concepción, Concepción, Chile}

[2] {Departmento de Oceanografía, Universidad de Concepción, Concepción, Chile}

[3] {Centro de Investigación Oceanográfica en el Pacífico sur-Oriental (COPAS Sur-Austral), Universidad de Concepción, Concepción, Chile}

[4] {Department of Earth, Atmospheric, and Planetary Sciences, Massachusetts Institute of Technology, Cambridge, MA, USA}

[5] {Facultad de Ciencias del Mar y Centro de Estudios Avanzados en Zonas Áridas (CEAZA), Universidad Católica del Norte, Coquimbo, Chile}

[6] {College of Earth, Ocean, and Atmospheric Sciences, Oregon State University, Corvallis, OR, USA}

[*]{now at: Department of Geological Sciences and Institute of Arctic and Alpine Research (INSTAAR), University of Colorado, Boulder, CO, USA}

Correspondence to: S. Pantoja (spantoja@udec.cl)

1 **Abstract**

2 We reconstructed oxygenation changes in the upwelling ecosystem off Concepción

3 (36ºS), Chile, using inorganic and organic proxies in a sediment core covering the last

4 ca. 110 years of sedimentation in this area. Authigenic enrichments of Mo, U and Cd

5 were observed between ca. 1935 and 1971 CE implying a prolonged period with

6 predominantly more reduced conditions in bottom waters and surface sediments.

7 Significant positive correlations between redox-sensitive metals, algal sterols,

8 biomarkers of micro-aerophilic and anaerobic microorganisms, and archaeal glycerol

9 dialkyl glycerol tetraethers point to a tight coupling among bottom water O_2 depletion

10 and increased primary and export production. The time interval with low O_2 of ca. 35

11 years seems to follow low frequency inter-decadal variation of the Pacific Decadal

12 Oscillation, and may have resulted in O_2 depletion over the entire continental shelf off

13 Concepción. Taken together with the concurrent increase in sedimentary molecular

14 indicators of micro-aerophilic and anaerobic microbes, allow us to suggest that changes

15 in oxygenation of the water column are reflected by changes in microbial community.

16 This study can inform our understanding of ecological consequences to projected trends

17 in ocean deoxygenation.

18

19 Key words: Oxygen Minimum Zone, upwelling, organic biomarkers, redox sensitive

20 metals, microbial community, Pacific Decadal Oscillation, Chile

21

22   **1. Introduction**

23

24 Oxygen Minimum Zones (OMZs) are epipelagic and mesopelagic subsurface layers of

25 suboxic waters (e.g., ≤ 22 μM O_2) found along Eastern Boundary currents, Arabian Sea

1   and Equatorial Pacific, where upwelling of nutrient-rich waters promotes elevated

2   primary production and O_2 consumption through microbial respiration (Wyrtky, 1962;

3   Helly and Levin, 2004; Paulmier and Ruiz-Pino, 2009). Due to strong redox gradients

4   and reducing conditions, an active microbial community connects cycling of carbon,

5   nitrogen, sulfur and other elements (Lam et al., 2009; Canfield et al., 2010; Naqvi et al.,

6   2010; Ulloa et al., 2012; Wright et al., 2012). Waters overlying the continental shelf of

7   central-southern Chile become seasonally depleted in O_2 during austral spring and

8   summer when the area is fed by the poorly oxygenated Peru–Chile Countercurrent. In

9   austral autumn and winter shelf waters are oxygenated due to the input of Subantarctic

10 waters (Ahumada and Chuecas, 1979; Sobarzo et al., 2007). Inter-annual phenomena

11 such as El Niño Southern Oscillation (ENSO) can also affect oxygenation of south

12 Pacific waters (Blanco et al., 2002; Carr et al., 2002; Levin et al., 2002). In central-

13 southern Chile, the upper edge of the OMZ deepens during El Niño thus allowing

14 greater oxygenation of bottom waters (Gutiérrez et al., 2000; Neira et al., 2001;

15 Escribano et al., 2004). Analyzing a sedimentary record from northern Chile, Vargas et

16 al. (2007) related changes in coastal upwelling and biological production to variations in

17 the Pacific Decadal Oscillation (PDO), characterized by an ENSO-like interdecadal

18 variability in the Humboldt Current System. During the cool phase of PDO, primary

19 production intensifies in response to upwelling and fertilization of the upper ocean

20 (Mantua et al., 1997, 2002; Cloern et al., 2007), leading to enhanced O_2 consumption in

21 the water column (Wyrtky, 1962; Sarmiento et al., 1998; Helly and Levin, 2004). Since

22 patterns of biological production and oxygenation of the water column during PDO

23 cycles resemble those of ENSO (Vargas et al., 2007), we hypothesize that variations at

24 the scale of PDO promote chemical and biological changes in the OMZ off central-

25 southern Chile.

1

1.1. Trace metals as redox proxies

3

4   Past redox variations can be analyzed using trace elements in sediments since some

5   redox-sensitive metals are less soluble under reducing conditions resulting in authigenic

6   enrichment in low oxygen and high organic matter environments (Algeo and Maynard,

7   2004; McManus et al., 2005). This chemical behavior makes molybdenum (Mo),

8   uranium (U), and cadmium (Cd) valuable paleoredox and paleoproductivity proxies

9   (Calvert and Pedersen, 1993; Morford and Emerson, 1999; Crusius et al., 1996; Algeo

10   and Maynard, 2004).

11

12   Mo occurs primarily as soluble MoO_4^{2-} in oxygenated marine waters and its reduction to

13   particle reactive thiomolybdates ($MoO_xS_{4x}^{2-}$) under anoxia or molybdenum sulfide

14   (MoS_4^{2-}) under euxinia, result in authigenic enrichment of sedimentary Mo (Crusius et

15   al., 1996; Helz et al., 1996; Zheng et al., 2000; Vorlicek and Helz, 2002), thus indicative

16   of O_2-depleted environments. Uranium is mainly present as U (VI) that binds to

17   carbonate ions, forming $UO_2(CO_3)_3^{4-}$ in seawater. Reduction of U (VI) to U (IV) occurs

18   under suboxic conditions and at similar redox potentials that allow Fe(III) reduction to

19   Fe(II) (Cochran et al., 1986; Klinkhammer and Palmer, 1991 ; Chaillou et al., 2002;

20   McManus et al., 2005, 2006). Higher content of U relative to Mo indicates anoxic

21   depositional conditions (Algeo and Maynard, 2004; Tribovillard et al., 2006) whereas

22   equal contents of U, V and Mo indicate euxinic conditions in sediments as well as the

23   overlying water column (Algeo and Maynard, 2004; Tribovillard et al., 2006).

24

1 Cadmium is delivered to marine sediment mainly in association with sinking organic

2 matter (Piper and Perkins, 2004).   If sediments are reduced then Cd is authigenically

3 enriched, likely as sulfide (Rosenthal et al., 1995; Gobeil et al., 1997; Morford and

4 Emerson, 1999; Morford et al., 2001).

5

6 **1.2. Lipid biomarkers**

7

8 In the past decade, a diverse and active microbial community has been uncover in OMZ

9 waters off central and northern Chile (Stevens and Ulloa, 2008; Farías et al., 2009;

10 Quiñones et al., 2009; Canfield et al., 2010; Molina et al., 2010; Levipan et al., 2012;

11 Srain et al., 2015). Temporal and compositional variations in this microbial community

12 can be studied by analyzing their cell membrane lipids (biomarkers) preserved in the

13 sedimentary record, as demonstrated in other OMZ areas of the ocean (Schouten et al.,

14 2000a; Arning et al., 2008; Rush et al., 2012).

15

16 Lipid biomarkers are organic molecules occurring in recent and geological materials

17 that have chemical structures that record their biological origin (Brassell, 1992;

18 Schouten et al., 2000a; Hinrichs et al., 2003; Coolen et al. 2008; Talbot et al., 2014).

19 Biomarkers are relatively resistant to degradation and they can be indicators of a broad

20 group of organisms or of a specific genus or species, and as such, of their growing

21 environment (Table 1) (Brassell et al., 1986; Brocks and Pearson, 2005). Abundant

22 sedimentary sterols $C_{27}\Delta^5$, $C_{28}\Delta^5$, $C_{29}\Delta^5$ and $C_{30}\Delta^{22}$ (Volkman et al., 2003) are indicative

23 of algal primary and export production. The content and composition of isoprenoidal

1   glycerol dialkyl glycerol tetraethers (GDGTs) are used as indicators of ammonia

2   oxidation by marine pelagic archaea (De Long et al., 1998; Schouten et al., 2000b;

3   Turich et al., 2007; Lincoln et al., 2014), which are capable of nitrifying under low-O_2

4   conditions (Brandhorst, 1959; Carlucci & Strickland 1968; Ward & Zafiriou 1988;

5   Ward et al. 1989; Lipschultz et al. 1990).

6

7   Changes in sedimentary contents of bacterial hopanes and hopanols are related to

8   variations in bacterial groups (Rohmer et al., 1984; Ourisson and Albrecht, 1992; Innes

9   et al., 1998; Talbot et al., 2007). Occurrence of C_{27}-trisnorhopene is favored in anoxic

10   and euxinic environments, and during upwelling events (Grantham et al., 1980;

11   Schouten et al., 2001), and considered as an indicator of anaerobic microbial

12   degradation (Volkman et al., 1983; Duan et al., 1996; Duan, 2000; Peters et al., 2005).

13   C_{16}, C_{17}, and C_{18} mono-O-alkyl glycerol ethers (MAGEs) are present in fermentative

14   and sulfate reducing bacteria (Langworthy et al., 1983; Langworthy and Pond, 1986;

15   Ollivier et al., 1991), although these biological sources do not appear to be unique

16   (Hernández-Sanchez et al., 2014).

17

18   We studied redox-sensitive metals and organic biomarkers in ca. 110-year sedimentary

19   record from the OMZ within the upwelling ecosystem off Concepción, central-southern

20   Chile (36° S), to infer temporal changes in biological production and oxygenation of the

21   water column. Our goal was to assess whether the intensity of the OMZ has varied over

22   the past century in response to ocean/atmosphere circulation patterns, and whether this

23   is reflected in changes in microbial community

24

25   **2. Methods**

1

2.1 Sampling

3

The study site (Station 18; 36º30.8' S 73º7' W) is located in the coastal upwelling

ecosystem off central-southern Chile at ca. 18 nautical miles from the coast of

Concepción (Fig. 1). Sampling was carried out as part of the "Microbial Initiative in

Low Oxygen off Concepción and Oregon" (http://mi_loco.coas.oregonstate.edu), and

the Oceanographic Time Series Program (Station 18) of the Center for Oceanographic

Research in the eastern South Pacific (COPAS) at University of Concepción

(www.copas.udec.cl/eng/research/serie).

11

A 25 cm sediment core was collected at a water depth of 88 m during austral summer

(February 2009) using a GOMEX box corer onboard R/V Kay-Kay II. The top 5 cm

were sectioned onboard every 0.5 cm, whereas the rest of the core was sampled at 1cm

resolution. Samples were stored in glass petri plates and kept frozen at -18 ºC until

laboratory analysis. The water column was sampled monthly at Station 18 from January

2008 to November 2009 with Niskin bottles, and temperature, salinity, O_2, and

fluorescence of chlorophyll *a* data were obtained using a Seabird 25 CTDO.

Fluorescence data were transformed to concentration of chlorophyll *a* according to

Parsons et al. (1984). All water column data were obtained from the database of the

COPAS Center.

22

2.2 Sedimentary redox potential and organic carbon content

24

1   Redox potential was measured in the top 15 cm of the sediment core using a redox

2   potential sensor (Hanna) with an accuracy of ± 0.1mV. Sedimentary organic carbon

3   content was determined by high temperature oxidation using a NA 1500 Carlo Erba

4   elemental analyzer. Prior to organic carbon analysis, inorganic carbon was removed by

5   placing samples into silver cups with a drop of Milli-Q water and then fuming over

6   night with concentrated HCl. Samples were dried at 60°C for analysis.

7

8   **2.3 Geochronology**

9

10 Sedimentary ^{210}Pb activities were determined by Alpha spectrometry of its daughter

11 ^{210}Po using ^{209}Po as a yield tracer (Flynn, 1968). Activities were quantified until 1 σ

12 error was achieved in a Canberra Quad Alpha Spectrometer. Ages (CE, Common Era)

13 were established according to Constant Rate of Supply model (CRS, Appleby and

14 Oldfield, 1978), which considers unsupported ^{210}Pb inventories (^{210}Pbxs).

15 Geochronology of our sediment core was determined through radiocarbon

16 measurements on fish scales and the best fit age curves resulting from CRS model and

17 three ^{14}C control points from a longer core (VG06-2) retrieved in 2006 from the same

18 sampling site (Muñoz et al., 2012 and Supplement). Resulting ages were converted to

19 calendar years before present using calibration curve MARINE09 (Reimer et al., 2009)

20 and applying a regional marine reservoir correction (ΔR) of 137±164 years, 2σ

21 confidence interval (Table S1; Fig. 2).

22

23 **2.4 Trace metal analysis**

24

1   Trace metals Mo, U, and Cd were analyzed with an Agilent 7500ce Inductively Coupled

2   Plasma-Mass Spectrometer (ICP-MS), and aluminum (Al) was determined in a Perkin

3   Elmer Analyst 700 Atomic Absorption Spectrometer. Sediment samples and analytical

4   blanks (18.0 MΩ deionized water) were sequentially digested with suprapure HNO_3,

5   HCl, $HClO_4$, and HF. Accuracy and precision of measurements were assessed by

6   analyzing reference material MESS-3 from the National Research Council of Canada.

7   Excess metal (Me_{xs}) was calculated as $[Me_{sample}] - ((Me/Al)_{earth} \times [Al_{sample}])$. $(Me/Al)_{earth}$

8   corresponds to an average ratio for the Biobío and Itata rivers (Fig. 1) in central-

9   southern Chile (J. M. Muratli, personal communication, 2012) (Table S2).

10

11   **2.5 Gas chromatography-mass spectrometry (GC-MS) of biomarkers**

12

13   Extraction of lipid biomarkers (i.e., hopanes, hopanols, sterols, and mono-O-alkyl-

14   glycerol ethers – MAGEs) from sediments was carried out according to a modified

15   Bligh and Dyer (1959) procedure, substituting dichloromethane for chloroform. Freeze-

16   dried sediment samples (1–5 g) were sequentially extracted by ultra-sonication with 30

17   mL dichloromethane/methanol (1:3 v/v, 2X), (1:1 v/v, 1X), and dichloromethane (2X).

18   The lipid extract was concentrated with a rotary evaporator and dried with anhydrous

19   Na_2SO_4. Lipid extracts were then separated into four fractions by column

20   chromatography (30 cm length, 1 cm ID) filled with ca. 7 g deactivated silica gel.

21   Aliphatic hydrocarbons (F1) were eluted with 40mL hexane, ketones (F2) were eluted

22   with 50 mL toluene/hexane (1:3 v/v), alcohols (F3) with 50 mL ethyl-acetate/hexane

23   (1:9 v/v), and polar compounds (F4) were eluted with 35 mL ethyl-

24   acetate/methanol/hexane (4:4:1v/v). The alcohol fraction (F3) was derivatized with 80

25   µL BSTFA (N,O- bis(trimethylsilyl) trifluoracetamide) and 40 µL TMCS

1   (trimethylchlorosilane) at 70 ºC for 1 h before analysis. Samples were analyzed in an

2   Agilent 6890 GC series coupled to an Agilent 5972 MS. Hopanols, sterols and MAGEs

3   were analyzed with a 30 m DB-5 column (0.5 mm ID, 0.25 μm film thickness) using He

4   as carrier gas. Oven temperature program included: 60 ºC (2min) to 150 ºC at 15 ºC

5   min^{-1}, to 320 ºC (held 34.5min) at 4 ºC min^{-1}. Hopanes were analyzed in the aliphatic

6   hydrocarbon fraction (F1) using a 30 m HP- 5 column (0.32 mm ID, 0.25 μm film

7   thickness). GC oven temperature program was: 80 ºC (2min) to 130 ºC at 20 ºC min^{-1},

8   to 310 ºC at 4º C min^{-1}. The MS was operated in electron impact mode (70 eV) with the

9   ion source at 250 ºC. Mass spectra were acquired in both full scan mode (m/z range 40–

10   600, scan rate 2.6 s^{-1}) and selective ion-monitoring mode (SIM, m/z 191 for hopanes

11   and hopanols). Concentrations of alcohols and aliphatic hydrocarbons were based on

12   those of internal standards 1-nonadecanol and squalene.

13

14   **2.6 Analysis of glycerol dialkyl glycerol tetraethers (GDGTs) by High**

15   **Performance Liquid Chromatography – Atmospheric Pressure Chemical**

16   **Ionization – Mass Spectrometry (HPLC-APCI-MS)**

17

18   Sedimentary material was sequentially extracted by ultrasonication (3X) with methanol,

19   dichloromethane-methanol (1:1, v/v), and dichloromethane. Lipid extracts were

20   concentrated using a rotary evaporator and dried over a small Pasteur pipette filled with

21   combusted glass wool and anhydrous Na_2SO_4. Lipids were separated into non-polar and

22   polar fractions using a Pasteur pipette filled with activated Al_2O_3, after elution with

23   hexane/dichloromethane (9:1, v/v) and dichloromethane/methanol (1:1 v/v),

24   respectively. An aliquot of the polar fraction was dissolved in hexane/propanol (99:1

25   v/v), and filtered through a 0.45 μm PFTE filter. HPLC-MS analysis followed

1   methodologies described by Hopmans et al. (2000) and Liu et al. (2012), using an

2   Agilent Technologies 1200 Series HPLC equipped with an auto-sampler and a binary

3   pump, linked to a Q-TOF 6520 mass spectrometer via an atmospheric pressure chemical

4   ionization interface (Agilent Technologies). Samples were dissolved in 200 μL

5   hexane/isopropanol (99:1 v/v). GDGTs were separated using a Prevail Cyano column

6   (2.1×150mm, 3mm; Grace, USA) and maintained at 35 ºC and a flow rate of 0.25mL

7   min^{-1}. The elution program was: 5 min 100 % eluent A (hexane/isopropanol, 99:1, v/v),

8   followed by a linear gradient to 100 % eluent B (hexane/isopropanol, 90:10 v/v) for 35

9   min, and then held at 100 % eluent B for 5 min. Quantification of core GDGTs was

10   achieved by co-injection of samples with a C_{46}GDGT as internal standard (Huguet et

11   al., 2006).

12

13   **2.7 Statistical analysis**

14

15   Homogeneity of variances was assessed using the Levene's test, whereas normality was

16   determined using a Shapiro–Wilk test. Non-parametric Spearman correlations were

17   calculated between selected variables in order to determine statistical associations with

18   significance < 0.05 (Software Statistica, version 12).

19

20   **3. Results**

21

22   **3.1 Oceanographic setting of the study site**

23

24   During austral fall and winter (April to August), water temperature ranged between 11

25   and 12 ºC in the upper 20 m of the water column, and between 10 and 11 ºC below 65

1   m depth (Fig. S1a). Surface salinity varied between 32 and 33 above 20 m, and was 34

2   below this depth (Fig. S1b). Chlorophyll a concentration varied between 0.3 and 1.4 mg

3   m^{-3} with higher values in the top 20 m (Fig. S1c). Oxygen concentration varied between

4   170 and 205 µM in the top 20 m, and dropped to values lower than 22 µM (suboxia)

5   below 60 m depth (Fig. S1d). During austral spring and summer (September to March)

6   surface temperature ranged between 13 and 15 ºC, decreasing to 10 ºC below 84 m

7   depth (Fig. S1a). Salinity varied between 31 and 34.5 in the whole water column (Fig.

8   S1b). Chlorophyll a concentrations up to 53 mg m^{-3} were measured in surface waters

9   (Fig. S1c). Oxygen concentration ranged between 114 and 217 µM in surface waters.

10   Suboxic waters (i.e., < 22 µM) occur below ca. 20 m (Fig. S1d), which is significantly

11   shallower than in austral fall-winter.

12

13   Redox potential decreased from −176 mV at the water-sediment interface to −325 mV

14   below 3 cm, indicating predominance of reducing conditions in near-surface sediments

15   at the time of sampling during austral summer (Fig. S1e), consistent with the occurrence

16   of 5 µM O_2 in bottom waters (Fig. S1d). A surface fluff layer with a *Thioploca* mat was

17   observed at the sediment-water interface. Organic carbon content varied between 0.07

18   and 0.1 g (gdw)‾ (Fig. S1e).

19

20   **3.2 Geochronology**

21

22   Background $^{210}Pb_{xs}$ activity of 0.80 ± 0.02 dpm g^{-1} was reached at 23 cm in the core.

23   Geochronology from both $^{210}Pb_{xs}$ inventories and radiocarbon ages (Fig. 2; Table S1)

24   fitted an exponential decrease (r^2 0.99) due to sediment compaction (Fig. 2), allowing

25   adjusting older ages (Binford, 1990). A recent sedimentation rate of 0.24 ± 0.02 cm yr^{-1}

1   was estimated, representing ca. 110 years of sedimentation in our sediment core at

2   Station 18.

3

4   **3.3 Redox sensitive trace metals**

5

6   Redox sensitive metals are enriched in the interval ca. 1935–1971 CE (Fig. 3a–c; black

7   bar). Mo_{xs} content ranged between 2.5 and 6.5 ppm (Fig. 3a), showing a similar vertical

8   distribution as U_{xs} (1.1-4.1 ppm; Fig. 3b), and Cd_{xs} (0.8-1.9 ppm; Fig. 3c). Enrichments

9   of Mo_{xs}, U_{xs}, and Cd_{xs} exhibited a significant correlation among each other (R_s: p <

10   0.05; Table 2; Fig. S2) indicating more reducing conditions in bottom waters and

11   sediments at this time. In comparison, the periods 1905–1919 CE and 1979–2005 CE

12   showed lower contents of redox-sensitive metals (Fig. 3a–c; white bars), pointing to

13   presumably more oxygenated bottom waters and sediments.

14

15   **3.4 Algal sterols**

16

17   Sterols $C_{27}\Delta^5$, $C_{28}\Delta^5$, $C_{29}\Delta^5$ and $C_{30}\Delta^{22}$ were identified through the fragmentation

18   pattern of their trimethylsilyl (TMS) derivatives. The presence of $C_{27}\Delta^5$-sterol

19   cholesterol (m/z 458 $[M]^+$) was confirmed by detection of ions m/z 129, m/z 329 and

20   368. The $C_{28}\Delta^5$-sterol (m/z 472 $[M]^+$) showed ions of m/z 129, as well as m/z 343 and

21   m/z 382. The $C_{29}\Delta^5$-sterol (m/z 486 $[M]^+$) was identified by prominent ions m/z 357

22   and 396. Prominent ions m/z 69, m/z 271, m/z 359 and m/z 500 $[M]^+$ confirmed the

23   presence of $C_{30}\Delta^{22}$ dinosterol. Sterol contents ranged between 1,029 and 12,164 µg (g

24    $C_{org})^{-1}$ with maximum values in surface sediments (Fig. 4a). Sterols correlated

25   positively with U_{xs} (R_s: p < 0.05; Table 2; Fig. S3).

1

2 **3.5 Archaeal GDGTs**

3

4 GDGTs were identified by their molecular ion and elution pattern: GDGT-0 (1302

5 $[M + H]^+$), GDGT-I (1300 $[M + H]^+$), GDGT-II (1298 $[M + H]^+$), GDGT-III (1296 $[M +$

6 $H]^+$), and GDGT-V and GDGT-V' (1292 $[M + H]^+$ known as crenarchaeol and

7 crenarchaeol regioisomer). Content of GDGTs varied between 1094 and 5423 µg (g

8 $C_{org})^{-1}$ (Fig. 4b), with elevated values at the base core and between ca. 1947 and 1975

9 CE (Fig. 4b). GDGTs and U_{xs} contents correlated positively (R_s: $p < 0.05$; Table 2; Fig.

10 S4).

11

12 **3.6 Hopanoid composition and abundance**

13

14 C_{27}-trisnorhopene (22,29,30 trinorhop-17,(21)-ene) was identified based on its

15 molecular ion fragment m/z 368 $[M^+-2H^+]$ and fragments m/z 191 and 231 indicating

16 unsaturation in the ring system (Table 3). Three diploptene isomers were identified

17 according to their mass spectra, hop-13,18-ene, neohopene, and hop-22,29-ene (Table 3;

18 Fig. S5a). C_{30} hopene diploptene was identified based on its molecular ion (m/z 410

19 $[M^+]$) and diagnostic ions m/z 395, 299 and 191 (Table 3; Fig. S5a). A homologous

20 series of C_{31} to C_{35} hopanes with $\alpha\beta$ configuration were identified through m/z 191 in

21 the hydrocarbon fraction (Fig. S5a). Homohopanes C_{31} , C_{33} , C_{34} , and C_{35} were present

22 as epimers S and R (Fig. 5a, Table 3), whereas C_{32} hopane occurred as the single epimer

23 R (Table 3; Fig. S5a). C_{27} norhopene, and hopanes C_{30} and C_{31} were the only

24 compounds with $\beta\beta$ configuration (Table 3; Fig. S5a). C_{31} hopane showed the highest

1   relative abundance in the homohopane homologous series, with S and R $17\alpha,21\beta$

2   homohopane as the predominant one, followed by hopanes C_{33} and C_{34} (Fig. S5a).

3

4    $17\beta,21\beta$ hopanol (C_{30}), $17\beta,21\beta$ homohopanol (C_{31}), $17\beta,21\beta$ bishomohopanol

5   (C_{32}), and $17\beta,21\beta$ trishomohopanol (C_{33}) were identified by the characteristic ion m/z

6   191 and by their molecular ions ([M]$^+$ m/z 500, m/z 514, m/z 528, and m/z 542) (Table

7   3; Fig. S5b). Homologue C_{32} was the most abundant hopanol (Fig. S5b). C_{27}-

8   trisnorhopene ranged between 0.03 and 1.1 µg (g C_{org})$^{-1}$. Maximum values occurred

9   between ca. 1935 and 1971 CE (Fig. 4c), whereas minimum values were observed

10   during intervals 1905–1928 CE and 1980–2005 CE (Fig. 4c). C_{27}-trisnorhopene

11   correlated positively with U_{xs} and Cd_{xs} (R_s : $p < 0.05$; Table 2; Fig. S6). The profile of

12   C_{31} hopanol content varied between 1.1 and 3.7 µg (g C_{org})$^{-1}$, and reached the highest

13   value during 1935–1971 CE (Fig. 4d). Positive correlations among C_{31} hopanol, Mo_{xs},

14   and Cd_{xs} were observed (R_s: $p < 0.05$; Table 2; Fig. S7). In contrast, C_{32} hopanol

15   anticorrelated with C_{31} hopanol, U_{xs}, and Cd_{xs} (R_s: $p < 0.05$; Table 2; Fig. 4e; Fig. S8).

16

17   **3.7 Mono-O-alkyl glycerol ethers (MAGEs) indicators of fermentative and**

18   **sulfate reducing bacteria**

19

20   Mass spectra of MAGEs showed a base peak ion of m/z 205 characteristics of

21   monoalkyl glycerol-TMS compounds, which corresponds to cleavage between carbons

22   1 and 2 of glycerol moiety, and fragment m/z 445 [M+H-CH$_3$]$^+$ due to loss of methyl

23   group. We identified C_{16}-MAGE with molecular ion m/z 460 [M]$^+$, C_{17}-MAGE with

24   m/z 474 [M]$^+$, and C_{18}-MAGE with m/z 488 [M]$^+$. Content of MAGEs (sum of C_{16},

25   C_{17}, and C_{18} MAGEs) varied between 9 and 628 µg (g C_{org})$^{-1}$ (Fig. 4f). MAGEs content

1   remained low (50 μg (g C_{org})$^{-1}$) during 1901–1928 CE (Fig. 4f). From ca. 1935 CE,

2   MAGEs contents increased reaching the highest value in surface sediments (Fig. 4f).

3   MAGEs correlated positively with Mo_{xs} and Cd_{xs} (R_s: $p < 0.05$; Table 2; Fig. S9).

4

5   **4 Discussion**

6

7   **4.1 Patterns of redox depositional conditions, and primary and export**

8   **production**

9

10 We interpret variations in contents of sedimentary redox-sensitive metals as changes in

11 oxygenation of bottom waters and surface sediments. This interpretation agrees with

12 previous observations by Böning et al. (2009) and Muñoz et al. (2012) for the

13 continental shelf off Concepción, as well as with authigenic enrichments of U and Mo

14 over the Oregon shelf and Peru upwelling region associated with O_2 depletion and

15 increased primary production (Scholz et al., 2011, Erhardt et al., 2014).

16

17 Higher excess amounts of Mo, Cd and U during the period between 1935 and 1971

18 (Fig., 3a, b, c) indicate more reduced depositional conditions. Favorable conditions for

19 Mo and Cd authigenic enrichments are observed in bottom water and surface sediments

20 during the upwelling season when high primary production, low water column O_2, and

21 severe low redox-potential in surface sediments occur (Figs. S1c, d, and e;

22 www.copas.udec.cl/eng/research/serie). However, downcore distribution of these trace

23 metals could also reflect subtle changes in intensity of O_2 depletion over the continental

24 shelf off central-southern Chile. Thus, from ca. 1932 to 1951 CE, an increase in excess

1 Mo and Cd indicates redox potential favorable to sulfate reduction and HS⁻ production

2 at least in bottom waters and surface sediment (euxinic conditions). Since ca. 1957 to

3 1969 CE, an increase in excess U content, coincident with a decrease in excess Mo and

4 Cd, could indicate a transition to anoxia from previous euxinic conditions since U

5 enrichment begins when the redox potential reaches that for Fe-oxide reduction

6 (Cochran et al., 1986; Klinkhammer and Palmer, 1991). The observed temporal

7 variations in the redox-potential evidenced by those subtle changes in trace metals

8 enrichment could result in readjustment of the microbial community to changing redox

9 potential of the water column. However, correspondence of these conditions with

10 changes in organic biomarker patterns is not necessarily detected in sediments since we

11 assume that sediment diagenesis is constant for organics but not for redox-sensitive

12 metals once they reach the sediments.

13

14 Downcore distribution of inorganic and organic proxies reveal a period of ca. 35 years

15 between ca. 1935 and 1971 CE (Figs. 3 and 4; black bar) when values of redox-sensitive

16 metals (Fig. 3), sterols (Fig. 4a), GDGTs (Fig. 4b), C_{27} trisnorhopene (Fig. 4c), C_{31}

17 hopanol (Fig. 4d), and MAGEs (Fig. 4f) were elevated. Taken together, these patterns

18 allow us to infer that water column O_2 was comparatively lower than during the periods

19 immediately before and after, in association with enhanced primary production based on

20 the observed increase of sterols and GDGTs contents (Fig. 4a). The two periods with

21 relatively more oxygenated conditions (ca. 1901 and 1919 CE, and ca. 1979 and 2000

22 CE; Figs. 3 and 4) are characterized by low metal enrichments (Fig. 3), a lower content

23 of bacterial biomarkers related to oxygen depleted conditions such as C_{27} trisnorhopene,

24 C_{31} hopanol, and MAGEs (Table 2; Figs. 4c, d and f), and lower organic matter export

25 as evidenced by low contents of sedimentary sterols (Fig. 4a) and GDGTs (Fig. 4b).

1

2 We suggest that for the period 1935–1971 CE algal export production was elevated, and

3 that this export is responsible for the increase in phytoplankton sterols (Fig. 4a), which

4 was concurrent with an increase in Cd (Fig. 3) and GDGTs (Fig. 4b). An enhanced

5 sinking of organic matter leads to a subsequent increase in the rate of O_2 consumption

6 by microbial degradation, potentially depleting O_2 in the water column (Helly and

7 Levin, 2004; Canfield, 2006) and sediments. Such conditions lead to Mo, U and Cd

8 enrichment in sediments. Higher GDGTs abundance during this time (Fig. 4b) may

9 reflect a better preservation of archaeal biomarkers favored by O_2 depletion as

10 demonstrated by Schouten et al. (2004) and Zonneveld et al. (2010). The positive

11 correlation between sterols, GDGTs, and U enrichments (Table 2) support this

12 conclusion, since U enrichment occurs in environments with low O_2 concentration

13 and/or high organic matter deposition (Dezileau et al., 2002; Böning et al., 2009;

14 Tribovillard et al., 2006; Muñoz et al., 2012).

15

16 **4.2 Changes in microbial communities in response to redox variation**

17

18 Hopanols C_{31} and C_{32} are used to analyze changes in the bacterial community structure

19 because they are the diagenetic products of bacteriohopanetetrols (BHPs), which in turn

20 can have different bacterial sources (Talbot et al., 2003). Hopanol content was

21 dominated by C_{32} hopanol, as found previously in recent sediments (Buchholz et al.,

22 1993; Innes et al., 1997, 1998; Talbot et al., 2003). C_{31} hopanol content was more

23 elevated between ca. 1935 and 1971 CE (Fig. 4d) with peaks at the beginning and end

24 of the low-O_2 period, and exhibited positive correlation with Mo_{xs} and Cd_{xs} (R_s: $p <$

25 0.05; Table 2). Content of C_{32} hopanol (Fig. 4e), a diagenetic product of BHTs (Innes

1   et al., 1998; Talbot et al., 2003), mostly produced by heterotrophic aerobic bacteria

2   (Rohmer et al., 1984), displays a common peak with C_{31} hopanol (Fig. 4d) between

3   1920 and 1935 and are decoupled thereafter, concurrent with enrichment of redox-

4   sensitive metals (Figs. 3a, b and c). Observed changes in abundance and distribution of

5   C_{31} and C_{32} hopanols, in concomitance with past variations of O_2 in the water column at

6   the study site, are consistent with previous findings by Saenz et al. (2011) and Kharbush

7   et al. (2013). These authors found that the composition and abundance of BHPs, the

8   biological sources of hopanoids, change with decreasing O_2 in the water column of the

9   Peruvian margin, Arabian Sea, Cariaco Basin, and in the Eastern Tropical North Pacific.

10

11   Trisnorhopanes are bacterial lipid markers associated with upwelling and anoxic

12   depositional environments, although their biological sources have not yet been

13   identified (Schouten et al., 2001; Peters et al., 2005). The highest C_{27} trisnorhopene

14   (Fig. 4c) content occurred during the proposed period of high primary production and

15   O_2 depletion (1935−1971 CE), suggesting a relationship between its abundance and

16   upwelling-favorable conditions and anaerobic bacterial activity, as previously suggested

17   for other areas of the world (Grantham et al., 1980; Duan et al., 1996; Duan, 2000;

18   Schouten et al., 2001).

19

20   Sedimentary content of MAGEs was also higher in the period 1935–1971 CE and in the

21   topmost sediments (Fig. 4f), resembling C_{16}-MAGE (Fig. 5 of Arning et al., 2008) at

22   the same sampling site (Station 18), assuming similar sedimentation rate as in our

23   core. MAGEs have been detected in sediments from upwelling regions of Namibia,

24   Peru, and central-southern Chile and are attributed to the occurrence of sedimentary

25   sulfate reducing bacteria (Arning et al., 2008). The presence of sulfate reducing

1   bacteria has been previously documented in coastal waters off Chile (Canfield et al.,

2   2010) and Peru (Finster and Kjeldsen, 2010).

3

4   **4.3 Forcing mechanisms and variations in OMZ intensity in central-**

5   **southern Chile**

6

7   Combined records of redox-sensitive metals and biomarkers suggest the occurrence of

8   enhanced reducing conditions at the sediment– water interface and likely in the water

9   column, from ca. 1935 until 1971 CE (Figs. 3 and 4), that roughly coincide with a cool

10   (negative) phase of the Pacific Decadal Oscillation (PDO) (Fig. 4g). This suggests a

11   link between changes in continental shelf oxygenation off Concepción and the PDO,

12   with alternating phases of decreased (1901–1930 and 1979–1997 CE) and enhanced

13   upwelling (ca. 1935 to 1971 CE). PDO is a recurring pattern of ocean– atmosphere

14   variability with phases that last between two and three decades (Mantua et al., 1997,

15   2002). During cool or negative phases, the western Pacific becomes warmer while parts

16   of the eastern Pacific become colder. The reverse pattern occurs during warm or

17   positive phase. PDO plays a major role in decadal-scale oceanographic variability in the

18   Pacific Ocean (Mantua et al., 1997, 2002; White and Cayan, 1998; Johnson and

19   McPhaden, 1999).

20

21   Negative correlations between sedimentary C_{27}-trisnorhopene, C_{31} hopanol, MAGEs,

22   and PDO values (Table 2; Fig. S10) and a positive correlation between C_{32} hopanol

23   (Table 2; Fig. S10) and PDO suggest that this basin-wide climatic anomaly has an

24   impact on local oceanographic conditions off Concepción, which in turn modulate

25   the structure of the microbial community. Bacterial C_{31} hopanol and MAGEs derive

1 from microorganisms associated with marked chemoclines and redox gradients

2 (Rohmer et al., 1984; Innes et al., 1997, 1998; Talbot et al., 2003, 2007; Kool et al.,

3 2014). Thus, positive PDO phases (warm) were likely associated with a decrease in

4 wind-driven upwelling, greater oxygenation, decreased primary productivity, and

5 a concomitant decrease of microorganisms associated with low O_2. Reverse

6 conditions must have dominated during negative PDO phases, with enhanced

7 upwelling and primary production. An increase in coastal upwelling off

8 Concepción, as expected during cool (negative) PDO phases, could contribute to

9 accumulation of atmospheric greenhouse gases as reported for upwelling

10 ecosystems at seasonal scales (Bakun and Weeks, 2004; Naqvi et al., 2010).

11

12 **5. Conclusions**

13

14 Our main goal was to assess the use of redox-sensitive metals and organic biomarkers in

15 the sedimentary record on the shelf off Concepción, Chile (36° S) as proxies for changes

16 in the intensity of the OMZ over the past century. Our conclusions are as follows:

17

18 1. Sedimentary redox-sensitive metals and organic biomarkers indicate interdecadal

19   variations in intensity (oxygenation) of the OMZ during the last 110 years.

20

21 2. Inorganic and organic sedimentary proxies reveal that enhanced O_2-depleted

22   conditions dominated from ca. 1935 to 1971 CE in synchronicity with

23   enhanced productivity and microbial activity, likely due to more favorable

24   conditions for the development of upwelling events.

3. We suggest that variations in the PDO could be the physical mechanism controlling interdecadal variations in redox conditions and composition of microbial community in the coastal upwelling ecosystem off Concepción. Negative (positive) phases of PDO correlate with decreased (enhanced) oxygenation on the continental shelf off Concepción.

References

Ahumada, R. and Chuecas, L.: Algunas características hidrográficas de la Bahía

Concepción (36º40' S–73º02'W) y áreas adyacentes, Chile, Gayana Miscelánea (Chile),

8, 1–56, 1979.

Algeo, T. J. and Maynard, J. B.: Trace-element behavior and redox facies in core shales

of Upper Pennsylvanian Kansas-type cyclothems, Chem. Geol., 206, 289–318, 2004.

Arning, E. T., Birgel, D., Schulz-Vogt, H. N., Holmkvist, L., Jorgensen, B. B., Larson,

A., and Peckman, J.: Lipid biomarker patterns of phosphogenic sediments from

upwelling regions, Geomicrobiol. J., 25, 69–82, 2008.

Appleby, P. G. and Oldfield, F.: The calculation of lead-210 dates assuming a constant

rate of supply of unsupported 210Pb to the sediment, Catena, 5, 1–8, 1978.

1 Bakun, A., and Weeks, S. J.: Greenhouse gas buildup, sardines, submarine eruptions,

2 and the possibility of abrupt degradation of intense marine upwelling ecosystems,

3 Ecological Letters, 7, 1015–1023, 2004.

4

5 Binford, M.: Calculation and uncertainty analysis of 210Pb dates for PIRLA project

6 lake sediments cores, J. Paleolimnol., 3, 253–267,1990.

7

8 Bligh, E. G. and Dyer, W. J.: A rapid method of total lipid extraction and purification,

9 Can. J. Biochem. Phys., 37, 911–917, 1959.

10

11 Blanco, J. L., Carr, M. E., Thomas, A. C., and Strub, P. T.: Hydrographic conditions off

12 northern Chile during the 1996–1998 La Niña and El Niño events, J. Geophys. Res.,

13 107, 3-1–3-3, 2002.

14

15 Böning, P., Brumsack, H. J., Schnetger, B., and Grunwald, M.: Trace element

16 signatures of Chilean upwelling sediments at ~ 36ºS, Mar. Geol., 259, 112–121, 2009.

17

18 Brandhorst, W.: Nitrification and denitrification in the eastern tropical North Pacific,

19 ICES Journal of Marine Sciences, 25, 3-20,1959.

20

21 Brassell, S. C., Eglinton, G., and Mo, F. J.: Biological marker compounds as indicators

22 of the depositional history of the Maoming oil shale. Organic Geochemistry 10: 927-

23 941, 1986.

24

1   Brassell, S. C.: Biomarkers in sediments, sedimentary rocks and petroleums: biological

2   origins, geological fate and applications. In: Geochemistry of organic matter in

3   sediments and sedimentary rocks., L.M. Pratt, Comer, J.B. and Brassell, S.C. (eds).

4   SEPM: Oklahoma, USA, 1992.

5

6   Brocks, J. J., and Pearson, A.: Building the Biomarker Tree of Life. Reviews in

7   Mineralogy and Geochemistry 59: 233-258, 2005.

8   Buchholz, B., Laczko, E., Pfennig, N., Rohmer, M., and Neunlist, S.: Hopanoids of a

9   recent sediment from Lake Constance as eutrophication markers, FEMS Microbiol.

10   Ecol., 102, 217– 223, 1993.

11

12   Calvert, S. E. and Pedersen, T. F.: Geochemistry of recent oxic and anoxic sediments:

13   implications for the geological record. Mar. Geol. 113, 67–88, 1993.

14

15   Canfield, D. E.: Models of oxic respiration, denitrification and sulfate reduction in

16   zones of coastal upwelling, Geochim. Cosmochim. Ac., 70, 5753–5765, 2006.

17

18   Canfield, D. E., Stewart, F. J., Thamdrup, B., De Brabandere, L., Dalsgaard, T.,

19   DeLong, E. F., Revsbech, N. P., and Ulloa, O.: A cryptic sulfur cycle in oxygen-

20   minimum-zone waters off the Chilean coast, Science, 330, 1375–1378, 2010.

21

Carlucci, A. F., and Strickland, J. D. H.: The isolation, purification and some kinetic studies of marine nitrifying bacteria, Journal of Experimental Marine Biology and Ecology, 2, 156-166, 1968.

Carr, M. E., Strub, P. T., Thomas, A., and Blanco, J. L.: Evolution of 1996–1999 La Niña and El Niño conditions off the western coast of South America: a remote sensing perspective, J. Geophys. Res., 107, 29-1–29-16, 2002.

Chaillou, G., Anschutz, P., Lavaux, G., Schäfer, J., and Blanc, G.: The distribution of Mo, U, and Cd in relation to major redox species in muddy sediments of the Bay of Biscay. Mar. Chem. 80, 41–59, 2002.

Cloern, J. M., Jassby, A. D., Thompson, J, K., and Hieb, K. A.: A cold phase of the East Pacific triggers new phytoplankton blooms in San Francisco Bay, P. Natl. Acad. Sci. USA, 104, 18561–18565, 2007.

Cochran, J. K., Carey, A. E., Sholkovitz, E. R., and Suprenant, L. D.: The geochemistry of uranium and thorium in coastal marine sediments and sediment porewaters, Geochim. Cosmochim., Acta, 50, 663–680, 1986.

Coolen M. J. L., Talbot H. M., Abbas B. A., Ward C., Schouten S., Volkman J. K., and Sinninghe Damsté, J. S.: Sources for sedimentary bacteriohopanepolyols as revealed by 16S rDNA stratigraphy, Environmental Microbiology, 10, 1783–1803, 2008.

1   Cornejo, M., Farías, L., and Gallegos, M.: Seasonal cycle of N_2O vertical distribution

2   and air-sea fluxes over the continental shelf waters off central Chile (36 S), Prog.

3   Oceanogr., 75, 383–395, 2007.

4

5   Crusius, J., Calvert, S., Pedersen, T., and Sage, D.: Rhenium and molybdenum

6   enrichments in sediments as indicators of oxic, suboxic, and sulfidic conditions of

7   deposition. Earth Planet. Sci. Lett. 145, 65–78, 1996.

8

9   DeLong, E. F., King, L. L., Massana, R., Cittone, H., Murray, A., Schleper, C., and

10   Wakeham, S. G.: Dibiphytanyl ether lipids in nonthermophilic crenarchaeotes, Appl.

11   Environ. Microb., 64, 1133–1138, 1998.

12

13   Dezileau, L., Bareilleb, G., and Reyss, J. L.: Enrichissement en uranium authigènedans

14   les sédiments glaciaires de l'océan Austral, CR Geosci., 334, 1039–1046, 2002.

15

16   Duan, Y., Luo, B., Xu, Y., and Ma, L.: Composition and geochemical significance of

17   biomarkers in marine sediments from Nansha Islands waters, the South China Sea,

18   Chin. J. Oceanol. Limn., 27, 258–263, 1996.

19

20   Duan, Y.: Organic geochemistry of recent marine sediments from the Nansha Sea,

21   China, Org. Geochem., 31, 159–167, 2000.

22

1 Erhrardt, A. M., Reimers, C. E., Kadko, D., and Paytan, A.: Records of trace metals in

2 sediments from the Oregon shelf and slope: investigating the occurrence of hypoxia

3 over the past several thousand years, Chem. Geol., 382, 32–43, 2014.

4

5 Escribano, R., Daneri, G., Farías, L., Gallardo, V. A., González, H. E., Gutiérrez, D.,

6 Lange, C. B., Morales, C. E., Pizarro, O., Ulloa, O., and Braun, M.: Biological and

7 chemical consequences of the 1997–1998 El Niño in the Chilean coastal upwelling

8 system: a synthesis, Deep-Sea Res. Pt. II, 51, 2389–2411, 2004.

9

10 Farías, L., Fernández, C., Faúndez, J., Cornejo, M., and Alcaman, M. E.:

11 Chemolithoautotrophic production mediating the cycling of the greenhouse gases N2O

12 and CH4 in an upwelling ecosystem, Biogeosciences, 6, 3053–3069, doi:10.5194/bg-6-

13 3053-2009, 2009.

14

15 Farrimond, P., Griffiths, T., and Evdokiadis, E.: Hopanoic acids in Mesozoic

16 sedimentary rocks: their origin and relationship with hopanes, Organic Geochemistry,

17 33, 965– 977, 2002.

18

19 Finster, K. W. and Kjeldsen, K. U.: Desulfovibrio oceani subsp. oceani sp. nov., subsp.

20 nov., and Desulfovibrio oceani subsp. galateae subsp. nov., novel sulfate-reducing

21 bacteria isolated from the oxygen minimum zone off the coast of Peru, A. Van Leeuw.

22 J. Microb., 97, 221–229, 2010.

23

24 Flynn, W. W.: The determination of low levels of polonium-210 in environmental

25 materials, Anal. Chim. Acta, 43, 221–227, 1968.

1

2   Grantham, P. J. and Douglas, A. G.: The nature and origin of sesquiterpenoids in some

3   Tertiary fossil resins, Geochim. Cosmochim. Ac., 44, 1801–1810, 1980.

4

5   Gobeil, C., MacDonald, R.W., and Sundby, B.: Diagenetic separation of cadmium and

6   manganese in suboxic continental margin sediments. Geochim. Cosmochim. Acta 61,

7   4647–4654, 1997.

8

9   Gutiérrez, D., Gallardo, V. A., Mayor, S., Neira, C., Vásquez, C., Sellanes, J., Rivas,

10   M., Soto, A., Carrasco, F., and Baltazar, M.: Effects of dissolved oxygen and fresh

11   organic matter on the bioturbation potential of macrofauna in sublittoral sediments off

12   central Chile, during the 1997–98 El Niño, Mar. Ecol. Prog. Ser., 202, 81–99, 2000.

13

14   Helly, J. J. and Levin, L. A.: Global distribution of naturally occurring marine hypoxia

15   on continental margins, Dee Sea Res. Pt. I, 51, 1159–1168, 2004.

16

17   Helz, G. R., Miller, C. V., Charnock, J. M., Mosselmans, J. F. W., Pattrick, R. A. D.,

18   Garner, C. D., and Vaughan, D. J.: Mechanism of molybdenum removal from the sea

19   and its concentration in black shales: EXAFS evidence, Geochim. Cosmochim. Ac., 60,

20   3631-3642, 1996.

21

22   Hernandez-Sanchez, M. T., Homoky, W. B., and Pancost, R. D.: Ocurrence of 1-O-

23   monoalkyl glycerol ether lipids in ocean waters and sediments, Org. Geochem., 66, 1–

24   13, 2014.

25

1 Hinrichs, K.-U., Hmelo, L. R., and Sylva, S. P.: Molecular fossil record of elevated

2 methane levels in late pleistocene coastal waters, Science, 299, 1214–1217, 2003.

3

4 Hopmans, E. C., Schouten, S., Pancost, R. D., van der Meer, M. T. J., and Sinninghe

5 Damsté, J. S.: Analysis of intact tetraether lipids in archaeal cell material and sediments

6 by high performance liquid chromatography/atmospheric pressure chemical ionization

7 mass spectrometry. Rapid Communication in Mass Spectrometry, 14, 585-589, 2000.

8

9 Huguet, C., Hopmans, E. C., Febo-Ayala, W., Thompson, D. H., Sinninghe Damsté, J.

10 S., and Schouten, S.: An improved method to determine the absolute abundance of

11 glycerol dibiphytanyl glycerol tetraether ipids, Org. Geochem., 37, 1036–1041, 2006.

12

13 Innes, H. E., Bishop, A. N., Head, I. M., and Farrimond, P.: Preservation and diagenesis

14 of hopanoids in recent lacustrine sediments of Priest Pot, England, Org. Geochem., 26,

15 565– 576, 1997.

16

17 Innes, H. E., Bishop, A. N., Fox, P. A., Head, I. M., and Farrimond, P.: Early diagenesis

18 of bacterio-hopanoids in recent sediments of Lake Pollen, Norway, Org. Geochem., 29,

19 1285– 1295, 1998.

20

21 Johnson, G. C. and McPhaden, M. L.: Interior pycnocline flow from the subtropical to

22 the equatorial Pacific Ocean, J. Phys. Oceanogr., 29, 3073–3089, 1999.

23

24 Kharbush, J. J., Ugalde, J. A., Shane, L. H., Allen, E. E., and Aluwihare, L. I.:

25 Composite bacterial hopanoids and their microbial producers across oxygen gradients in

1   the water column of the California Current, Appl. Environ. Microb., 79, 7491–7501,

2   2013.

3

4   Klinkhammer, G. P., and Palmer, M. R.: Uranium in the oceans: where it goes and why,

5   Geochim. Cosmochim., Acta, 55, 1799–1806, 1991.

6

7   Kool, D. M., Talbot, H. M., Rush, D., Ettwing, K., and Sinninghe Damsté, J. S.: Rare

8   bacteriohopanepolyols as markers for an autotrophic, intra-aerobic methanotroph,

9   Geochimica et Cosmochimica Acta, doi: http//dx.doi.org/10.1016/j.gca.2014.04.002,

10   2014.

11

12   Lam, P., Lavik, G., Jensen, M. M., van de Vossenberg, J., Schmid, M., Woebken, D.,

13   Gutiérrez, D., Aman, R., jetten, M. S. M., and Kuypers, M. M.: Revising the nitrogen

14   cycle in the Peruvian oxygen minimum zone, Proceedings of the National Academy of

15   Sciences, 106, 4752–4757, 2009.

16

17   Langworthy, T. A., Holzer, G., Zeikus, J. G., and Tornabene, T. G.: Iso- and anteiso-

18   branched glycerol diethers of the thermophilic anaerobe Thermodesulfotobacterium

19   commune, Syst. Appl. Microbiol., 4, 1–17, 1983.

20

21   Langworthy, T. A. and Pond, J. L.: Archaebacterial ether lipids and chemotaxonomy,

22   Syst. Appl. Microbiol., 7, 253–257, 1986.

23

1   Levin, L. A., Rathburn, A. E., Neira, C., Sellanes, J., Muñoz, P., Gallardo, V., and

2   Salamanca, M.: Benthic processes on the Perú margin: a transect across the oxygen

3   minimum zone during the 1997–1998 El Niño, Prog. Oceanogr., 53, 1–27, 2002.

4

5   Levipan, H. A., Alarcón, W. O., and Saldías, G. S.: Fingerprinting analysis of the

6   prokaryote community along a marine-freshwater transect in central-southern Chile,

7   Ann. Microbiol., 62, 1121–1140, 2012.

8

9   Lincoln, S. A., Brenner, W., Eppley, J. M., Church, M. J., Summons, R. E., and

10   DeLong, E. F.: Planktonic Euryarchaeota are significant source of archaeal tetraether

11   lipids in the ocean, P. Natl. Acad. Sci. USA, 111, 9858–9863, 2014.

12

13   Lipschultz, F., Wofsy, S. C., Ward, B. B., Codispoti, L. A., Friedrich, G., and Elkins, J.

14   W.: Bacterial transformations of inorganic nitrogen in the oxygen-deficient waters of

15   the eastern tropical south Pacific Ocean, Deep Sea Research, 37, 1513-1541, 1990.

16

17   Liu, X., Summons, R. E., and Hinrichs, K. U.: Extending the known range of glycerol

18   ether lipids in the environment: structural assignments based on MS/MS fragmentation

19   patterns, Rapid Communications in Mass Spectrometry, 26, 2295-2302, 2012.

20

21   Mantua, N. J., Hare, S. R., Zhang, Y., Wallace, J. M., and Francis, R. C.: A Pacific

22   decadal climate oscillation with impacts on salmon, B. Am. Meteorol. Soc., 78, 1069–

23   1079, 1997.

24

1   Mantua, N. J. and Hare, S. R.: The Pacific Decadal Oscillation, J. Oceanogr., 58, 35–44,

2   2002.

3

4   McManus, J., Berelson, W. M., Klinkhammer, G. P., Hammond, D. E., and Holm, C.:

5   Authigenic uranium: relationship to oxygen penetration depth and organic carbon rain,

6   Geochim. Cosmochim. Ac., 69, 95–108, 2005.

7

8   McManus, J., Berelson, W. M., Severmann, S., Poulson, R. L., Hammond, D. E.,

9   Klinkhammer, G. P. and Holm, C.: Molybdenum and uranium geochemistry in

10 continental margin sediments: Paleoproxy potencial, Geochim. Cosmochim. Ac., 70,

11 4643-4662, 2006.

12

13 Molina, M., Belmar, L., and, Ulloa, O.: High diversity of ammonia-oxidizing archaea in

14 permanent and seasonal oxygen-deficient waters of the eastern South Pacific, Environ.

15 Microbiol., 12, 2450–2465, 2010.

16

17 Morford, J. L. and Emerson, S.: The geochemistry of redox sensitive trace metals in

18 sediments. Geochim. Cosmochim. Acta 63, 1735–1750, 1999.

19

20 Morford, J. L., Russell, A. D., and Emerson, S.: Trace metal evidence for changes in the

21 redox environment assocoated with the transition from terrigenous clay to diatomaceous

22 sediments, Saanich Inlet, BC. Mar. Geol. 174, 355–369, 2001.

23

1   Muñoz, P., Dezileau, L., Cardenas, L., Sellanes, J., Lange, C. B., Inostroza, J., Muratli,

2   J. J., and Salamanca, M.: Geochemistry of trace metals in shelf sediments affected by

3   seasonal and permanent low oxygen conditions off central Chile, SE Pacific ($\sim 36\circ$ S),

4   Cont. Shelf Res., 33, 51–68, 2012.

5

6   Naqvi, S. W. A., Bange, H. W., Farías, L., Monteiro, P. M. S., Scraton, M. I., and

7   Zhang, J.: Marine hypoxia/anoxia as source of CH_4 and N_2O, Biogeosciences, 7, 2159–

8   2190, 2010.

9

10 Neira, C., Sellanes, J., Soto, A., Gutierrez, D., and Gallardo, V. A.: Meiofauna and

11 sedimentary organic matter off Central Chile: response to changes caused by the 1997–

12 1998 El Niño, Oceanol. Acta, 24, 313–328, 2001.

13

14 Ollivier, B., Hatchikian, C. E., Prensier, G., Guezennec, J., and Garcia, J. L.:

15 Desulfohalobium retbaense gen. nov. sp. nov., a halophilic sulfatereducing bacterium

16 from sediments of a hypersaline lake in Senegal, Int. J. Syst. Bacteriol., 41, 74–81,

17 1991.

18

19 Ourisson, G. and Albrecht, P.: Hopanoids. 1. Geohopanoids: the most abundant natural

20 products on Earth?, Accounts Chem. Res., 25, 398–402, 1992.

21

22 Parsons, T. R., Maita, Y., and Lalli, C. M.: A Manual of Chemical and Biological

23 Methods for Seawater Analysis, Pergamon Press, Oxford, UK, 1984.

24

1   Paulmier, A. and Ruiz-Pino, D.: Oxygen minimum zones (OMZs) in the modern ocean,

2   Prog. Oceanogr., 80, 113–128, 2009.

3

4   Peters, K. E., and Moldowan J. M.: The Biomarker Guide, Prentice Hall, Engelwood

5   Cliffs, NJ., 1993.

6

7   Peters, K. E., Walters, C. C., and Moldowan, J. M.: The Biomarker Guide, 2nd edn.,

8   Volume II, Biomarkers and Isotopes in Petroleum Systems and Earth History,

9   Cambridge University Press, UK, 684 pp., 2005.

10

11   Piper, D. Z., and Perkins, R. B.: A modern vs. Permian black shale–the hydrography,

12   primary productivity, and water-column chemistry of deposition. Chem. Geol. 206,

13   177–197, 2004.

14

15   Quiñones, R. A., and Levipan, H. A.: Spatial and temporal variability of plaktonic

16   archaeal abundance in the Humboldt Current System off Chile, Deep-Sea Research Part

17   II, 56, 1073-1082, 2009.

18

19   Reimer, P. J., Baillie, M. G. L., Bard, E., Bayliss, A., Beck, J. W., Blackwell, P. G.,

20   Bronk, Ramsey, C., Buck, C. E., Burr, G. S., Edwards, R. L., Friedrich, M., Grootes, P.

21   M., Guilderson, T. P., Hajdas, I., Heaton, T. J., Hogg, A. G., Hughen, K. A., Kaiser, K.

22   F., Kromer, B., McCormac, F. G., Manning, S. W., Reimer, R. W., Richards, D. A.,

23   Southon, J. R., Talamo, S., Turney, C. S. M., van der Plicht, J., and Weyhenmeyer, C.

1   E.: IntCal09 and Marine09 radio- carbon age calibration curves, 0–50,000 years cal BP,

2   Radiocarbon, 51, 1111–50, 2009.

3

4   Rohmer, M., Bouvier-Nave, P., and Ourisson, G.: Distribution of hopanoid triterpenes

5   in prokaryotes, J. Gen. Microbiol., 130, 1137–1150, 1984.

6

7   Rosenthal, Y., Lam, P., Boyle, E.A., and Thomson, J.: Authigenic cadmium

8   enrichments in suboxic sediments: Precipitation and postdepositional mobility, Earth

9   and Planetary Science Letters, 132, 99-111, 1995.

10

11 Rush, D., Hopmans, E. C., Wakeham, S. G., Schouten, S., and Sinninghe Damsté, J. S.:

12 Occurrence and distribution of ladderane oxidation products in different oceanic

13 regimes, Biogeosciences, 9, 2407–2418, doi:10.5194/bg-9-2407-2012, 2012.

14

15 Saenz, J., Summons, R., Eglinton, T. I., and Wakeham, S. G.: Distribution of bacterio-

16 hopanepolyols in marine anoxic environments: new constraints on the provenance of

17 hopanoids in the marine geologic record, Org. Geochem., 42, 1322–1351, 2011.

18

19 Sarmiento, J. L., Hughes, T. M. C., Stouffer, R. J., and Manabe, S.: Simulated response

20 of the ocean carbon cycle to anthropogenic climate warming, Nature, 393, 245–249,

21 1998.

22

23 Scholz, F., Hensen, C., Noffke, A., Rohde, A., Liebetrau, V., and Wallmann, K.: Early

24 diagenesis of redox-sensitive trace metals in the Peru upwelling area response to ENSO-

1 related oxygen fluctuations in the water column, Geochimica, et Cosmochimica Acta,

2 75, 7257–7276, 2011.

3

4 Schouten, S., Hoefs, M. J. L., and Sinninghe Damsté, J. S.: A molecular and stable

5 carbon isotopic study of lipid in late quaternary sediments from the Arabian Sea, Org.

6 Geochem., 31, 509–532, 2000a.

7

8 Schouten, S., Hopmans, E. C., Pancost, R. D., and Sinninghe Damsté, J. S.: Widespread

9 occurrence of structurally diverse tetraether membrane lipids: evidence for the

10 ubiquitous presence of low-temperature relatives of hyperthermophiles, P. Natl. Acad.

11 Sci. USA, 97,14421–14426, 2000b.

12

13 Schouten, S., de Loureiro, M. R. B., Sinninghe Damsté, J. S., and de Leeuw, J. W.:

14 Molecular biogeochemistry of Monterrey sediments, Napoles Beach, California. I:

15 distributions of hydrocarbons and organic sulfur compunds, in: The Monterrey

16 Formation: From Rocks to Molecules, edited by: Isaacs, C. M. and Rullkötter, J.,

17 Columbia University Pres, New York, 150–174, 2001.

18

19 Schouten, S., Hopmans, E. C., and Sinninghe Damsteì, J. S.: The effect of maturity and

20 depositional redox conditions on archaeal tetraether lipid palaeothermometry, Org.

21 Geochem., 35, 567–571, 2004.

22

23 Sobarzo, M., Bravo, L., Donoso, D., Garcés-Vargas., J.,and Schneider, W.: Coastal

24 upwelling and seasonal cycles that influence the water column over the continental shelf

25 off central Chile, Progress in Oceanography, 75, 363–382, 2007.

1

2 Srain, B., Sepúlveda, J., Pantoja, S., Summons, R. E., Quiñones, R. A., and Levipan, H.

3 A.: Archaeal and bacterial assemblages in the Oxygen Minimum Zone of the upwelling

4 ecosystem off Central Chile as determined by organic biomarkers, International Journal

5 of Biodiversty, Oceanology and Conservation, 79, 2015.

6

7 Stevens, H. and Ulloa, O.: Bacterial diversity in the oxygen minimum zone of the

8 eastern tropical South Pacific, Environ. Microbiol., 10, 1244–1259, 2008.

9

10 Talbot, H. M. and Farrimond, P.: Bacterial populations recorded in diverse sedimentary

11 biohopanoid distributions, Org. Geochem., 38, 1212–1225, 2007.

12

13 Talbot, H. M., Watson, D. F., Murrell, J. C., Carter, J. F., and Farrimond, P.: Analysis

14 of intact bacteriohopanepolyols from methanotrophic bacteria by reversed-phase high-

15 performance liquid chromatography-atmospheric pressure chemical ionisation mass

16 spectrometry, J. Chromatogr. A, 921, 175−185, 2001.

17

18 Talbot, H. M., Watson, D. F., Pearson, E. J., and Farrimond, P.: Diverse biohopanoid

19 compositions of non-marine sediments, Org. Geochem., 34, 1353–1371, 2003.

20

21 Talbot, H., Rohmer, M., and Farrimond, P.: Rapid structural elucidation of composite

22 bacterial hopanoids by atmospheric pressure chemical ionization liquid

23 chromatography/ion trap mass spectrometry, Rapid Communications in Mass

24 Spectrometry, 21, 880-892, 2007.

25

1   Talbot, H. M., Handley, L., Spencer-Jones, C., Bienvenu, D. J., Schefuß, E., Mann, P.,

2   Poulson, J., Spencer, R., and Wagner, T.: Variability in aerobic methane oxidation over

3   the past 1.2 Myrs recorded in microbial biomarker signatures from Congo fan

4   sediments, Geochimica et Cosmochimica Acta, doi:10.1016/j.gca.2014.02.035, 2014.

5

6   Thiel, V., Blumenberg, M., Pape, T., Seifert, M., and Michaelis, W.: Unexpected

7   occurrence of hopanoids at gas seeps in the Black Sea, Organic Geochemistry, 34(1),

8   81–87, 2003.

9

10 Tribovillard, N., Algeo, T. J., Lyons, T., and Riboulleau, A.: Trace metals as paleoredox

11 and paleoproductivity proxies: an update, Chem. Geol., 232, 12–32, 2006.

12

13 Turich, C., Freeman, K. H., Bruns, M. A., Conte, M., Jones, A. D., and Wakeham, S.

14 G.: Lipids of marine Archaea: patterns and provenance in the water-column and

15 sediments, Geochim. Cosmochim. Ac., 71, 3272–3291, 2007.

16

17 Ulloa, O., Canfield, D. E., DeLong, E. F., Letelier, R. M., and Stewart, F. J.: Microbial

18 oceanography of anoxic oxygen minimum zones, P. Natl. Acad. Sci. USA, 109, 15996–

19 16003, 2012.

20

21 Vargas, G., Pantoja, S., Rutillant, J., Lange, C. B., and Ortlieb, L.: Enhancement of

22 coastal upwelling and interdecadal ENSO-like variability in the Peru-Chile Current

23 since late 19th century, Geophysical Research Letters, 34, L13607, doi:

24 10.1029/2006GL028812, 2007.

25

1   Venkatesan, M. I., Ruth, E., and Kaplan, I. R.: Triterpenols from sediments of Santa

2   Monica Basin, Southern California Bight, USA, Organic Geochemistry, 16, 1015–1024,

3   1990.

4

5   Volkman, J. K., Alexander, R., Kagi, R. I., and Rullkötter, J.: GC-MS characterization

6   of C27 and C28 triterpanes in sediments and petroleum, Geochim. Cosmochim. Ac., 47,

7   1033–1040, 1983.

8

9   Volkman, J. K.: Sterols in microorganisms, Applied Environmental Biotechnology, 60,

10   495–506, 2003.

11

12   Vorlicek, T. P. and Helz, G. R.:Catalysis by mineral surfaces: Implications for Mo

13   geochemistry in anoxic environments, Geochim. Cosmochim. Ac., 66, 3679-3692,

14   2002.

15

16   Ward, B. B., and Zafiriou, O. C.: Nitrification and nitric oxide in the oxygen minimum

17   zone of the eastern tropical North Pacific, Deep Sea Research, 35, 1127-1142, 1988.

18

19   Ward, B. B., Glover, H. E., and Lipschultz, F.: Chemoautotrophic activity and

20   nitrification in the oxygen minimum zone off Peru, Deep Sea Research, 36, 1031-1051,

21   1989.

22

23   White, W. B. and Cayan, D. R.: Quasi-periodicity and global symmetries in

24   interdecadal upper ocean temperature variability, J. Geophys. Res., 103, 21335–21354,

25   1998.

1

2 Wright, J. D., Kishori, M., Konwar, M., and Hallam, S. J.: Microbial ecology of

3 expanding oxygen minimum zones, Nat. Rev. Microbiol., 10, 381–394, 2012.

4

5 Wyrtki, K.: The oxygen minima in relation to ocean circulation, Deep-Sea Res., 9, 11–

6 23, 1962.

7

8 Zheng, Y., Anderson, R. F., van Geen, A., and Kuwabara, J.: Authigenic molybdenum

9 formation in marine sediments: a link to pore water sulfide in the Santa Barbara Basin.

10 Geochim. Cosmochim. Acta 64, 4165–4178, 2000.

11

12 Zonneveld, K. A. F., Versteegh, G. J. M., Kasten, S., Eglinton, T. I., Emeis, K. C.,

13 Huguet, C., Koch, B. P., de Lange, G. J., de Leeuw, J. W., Middelburg, J. J.,

14 Mollenhauer, G., Prahl, F. G., Rethemeyer, J., and Wakeham, S. G.: Selective

15 preservation of organic matter in marine environments; processes and impact on the

16 sedimentary record, Biogeosciences, 7, 483– 511, doi:10.5194/bg-7-483-2010, 2010.

17

18 **Figure captions**

19

20 Figure 1. Location of sampling site Station 18 in the upwelling ecosystem off

21 Concepción, central-southern Chile. Bathymetry in shades of blue, scale on right-hand

22 side.

23

1   Figure 2. Geochronology estimated from $^{210}Pb_{xs}$ inventories (black line) and ^{14}C

2   measurements ± standard deviation. Ages are years before present (1950). Dotted line

3   shows fitted values from curve ($r^2 = 0.99$).

4

5   Figure 3. Downcore excess content (ppm) of redox-sensitive metals a) Mo, b) U, and c)

6   Cd. Shaded area and black bar correspond to a period of ca. 35 years of enhanced

7   authigenic precipitation of redox-sensitive metals compared to periods of higher

8   oxygenation (white bars) and low authigenic precipitation. CE = Common Era. Samples

9   for interval 1957−1969 were lost.

10

11   Figure 4. Downcore contents of a) sterols, b) archaeal GDGTs, c) 17α-22,29,30-

12   trinorhopene (C_{27}-TNH), d) 17β,21β-homohopanol (C_{31} hopanol), e) 17β,21β-

13   bishomohopanol (C_{32} hopanol), f) MAGEs, and g) Pacific Decadal Oscillation (PDO)

14   index (http://jisao.washington.edu/pdo/PDO.latest). Units are micrograms per gram dry

15   weight. Shaded area and black bar as in Fig. 3. Gaps in the record indicate that

16   biomarker content was under detection limit.

17

18

19

20

21

22

23

24

25

1 **Figures**

2 **Figure 1**

3
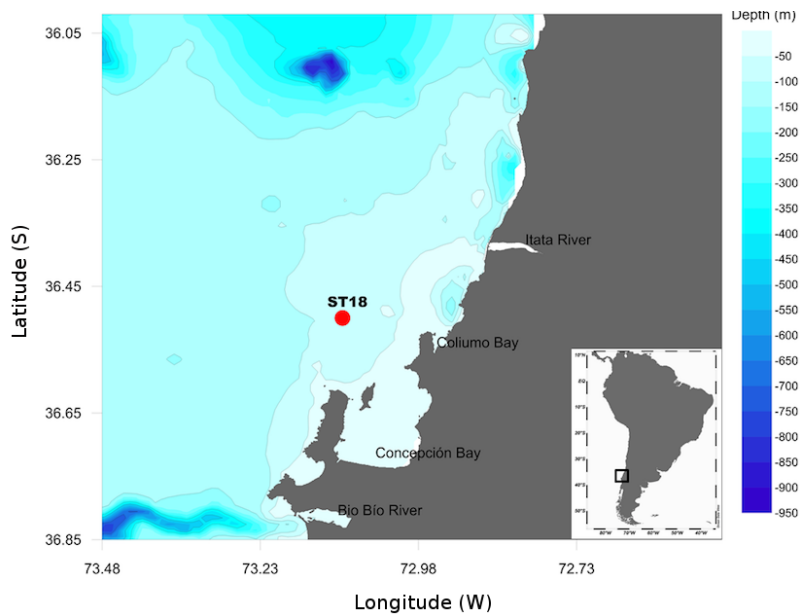
4

5

6 **Figure 2**

7

8

9

10

1   **Figure 3**

2

a) Mo$_{XS}$ (ppm)   b) Cd$_{XS}$ (ppm)   c) U$_{XS}$ (ppm)

3

4

5   **Figure 4**

6

a) Sterols (µg g (C$_{org}$)$^{-1}$)   b) GDGTs (µg g (C$_{org}$)$^{-1}$)   c) C$_{27}$ trisnorhopene (µg g (C$_{org}$)$^{-1}$)   d) C$_{31}$ hopanol (µg g (C$_{org}$)$^{-1}$)

e) C$_{32}$ hopanol (µg g (C$_{org}$)$^{-1}$)   f) MAGEs (µg g (C$_{org}$)$^{-1}$)   g) PDO Index

Running average
Annual average PDO

7

8
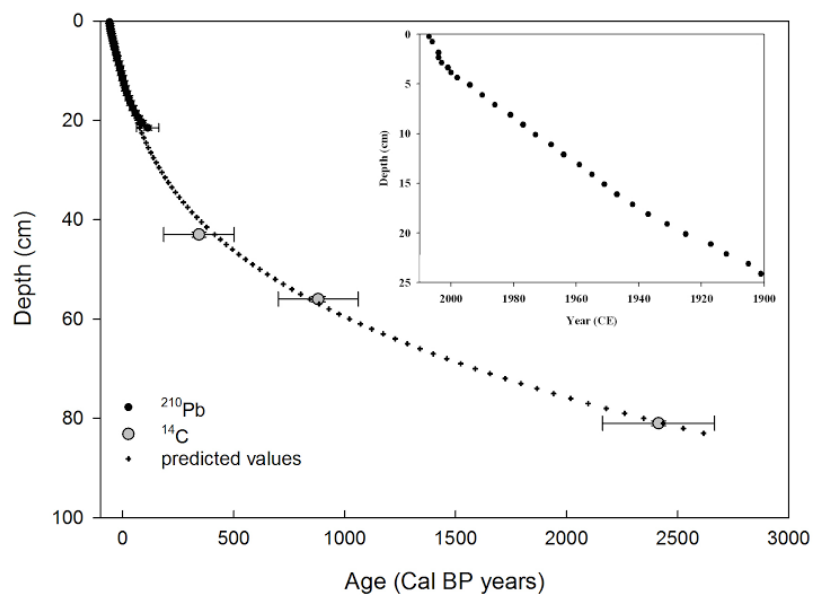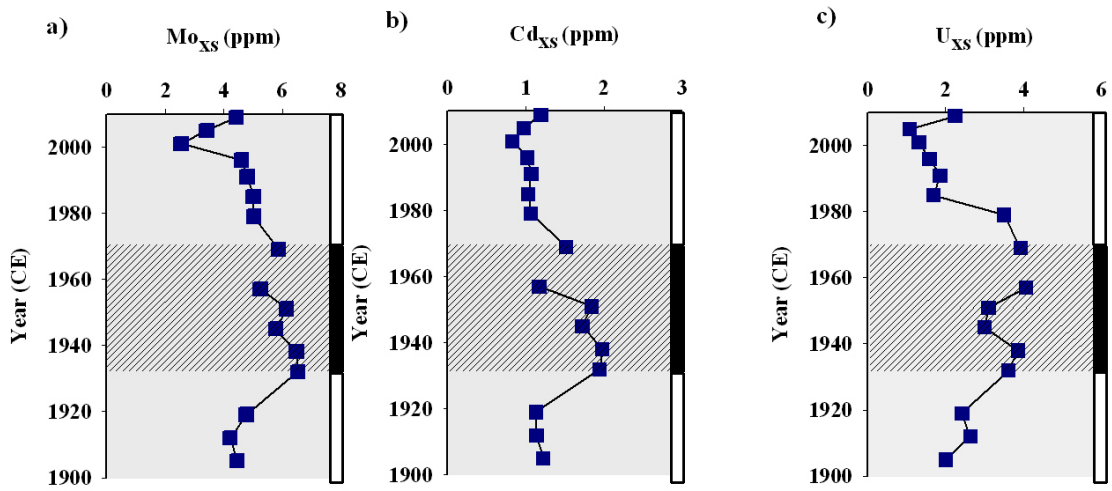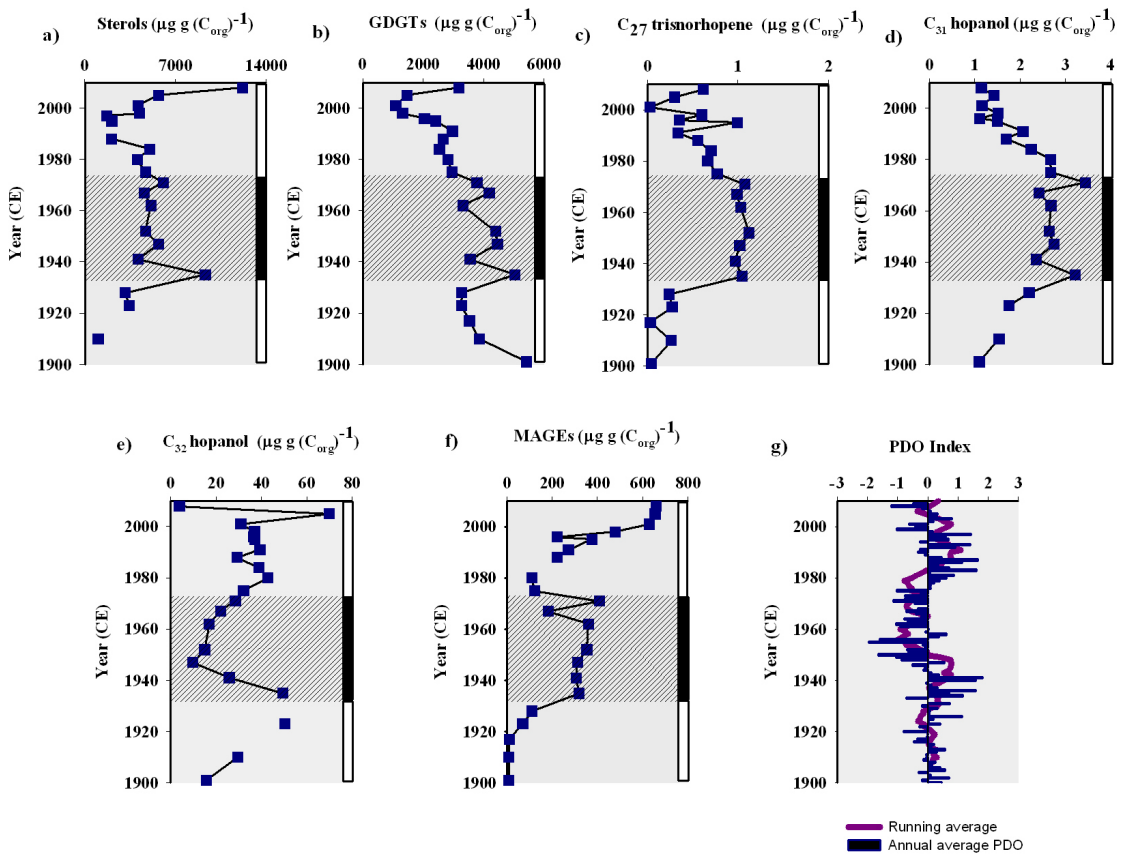
1 Tables

Table 1. Lipid biomarkers used in this study and their paleobiological interpretation

Biomarker	Biological and/or environmental interpretation	References
Hopanoids hydrocarbons		
C_{30} hopanes	Diverse bacterial lineages, few eukaryotic species (e.g. some cryptogams, ferns, mosses, lichens, filamentous fungi, protists)	Rohmer et al., 1984
Extended C_{31} to C_{35} hopanes (homohopanes)	Diagnostic for Bacteria. Its biosynthesis is restricted to facultative anaerobes and strict anaerobes involved in anaerobic methane cycling (Thiel et al., 2003)	Rohmer et al., 1984; Ourisson and Albrecht, 1992
22,29,30-trinor-hop-17(21)-ene (C_{27}-trisnorhopene)	Detected in anoxic and euxinic sediments, and during upwelling events, and considered indicator of anaerobic microbial degradation	Grantham et al., 1980; Volkman et al., 1983; Peters and Moldowan, 1993; Schouten et al., 2001
Hopanols		
$17\beta,21\beta$-hopanol (C_{30})	Diverse bacterial lineages. Diagenetic product of hexafunctionalized bacteriohopanepolyols	Rohmer et al., 1984; Venkatesan et al., 1990; Innes et al., 1997, 1998; Talbot et al., 2001; Farrimond et al., 2002
$17\beta,21\beta$-homohopanol (C_{31})	Diverse bacterial lineages. Diagenetic product of pentafunctionalized bacteriohopanepolyols	Rohmer et al., 1984; Venkatesan et al., 1990; Innes et al., 1997, 1998; Talbot et al., 2001; Farrimond et al., 2002
$17\beta,21\beta$-bishomohopanol (C_{32})	Diverse bacterial lineages. Diagenetic product of bacteriohopanetetrols	Rohmer et al., 1984; Venkatesan et al., 1990; Innes et al., 1997, 1998; Talbot et al., 2001; Farrimond et al., 2002
Sterols		
$C_{27}\Delta^5$	Bacillariophyceae, Bangiophyceae Dinophyceae, marine Eustigmatophyceae, Haptophyceae. Indicator of primary production and algal bloom.	Volkman, 2003
$C_{29}\Delta^5$	Diverse microalgae lineages (Bacillariophyceae, Chlorophyceae, Chrysophyceae, Euglenophyceae, Haptophyceae, Pelagophyceae, Raphidophyceae, Xanthophyceae). Indicator of primary production and algal bloom	Volkman, 2003
$C_{30}\Delta^{22}$	Dinophyceae	Volkman, 2003
MAGEs		
C_{16}-MAGE to C_{18}-MAGE	Fermentative and sulfate reducing bacteria. Biological source does not appear unique. Considered indicators of suboxic/anoxic water column and sediments	Langworthy et al., 1983; Langworthy and Pond, 1986; Ollivier et al., 1991; Hernández-Sanchez et al., 2014
GDGTs		
GDGT-0 to GDGT-V	Marine archaea (Thaumarchaeota and Euryarchaeota). Considered indicators of ammonia oxidation by Thaumarchaeota and archaeal secondary production	DeLong et al., 1998; Schouten et al., 2000b; Turich et al., 2007; Lincoln et al., 2014

Table 2. Spearman rank order correlations. Significant values ($p<0.05$) are highlighted in bold.

	Mo_{xs}	U_{xs}	Cd_{xs}	Sterols	GDGTs	C_{27} trisnorhopane	C_{31} hopanol	C_{32} hopanol	MAGEs	PDO Index
Mo_{xs}		**0.6**	**0.6**	0.2	0.3	0.2	**0.6**	-0.3	**0.6**	**-0.3**
U_{xs}	**0.6**		**0.5**	**0.4**	**0.6**	**0.5**	0.4	**-0.5**	**0.4**	-0.3
Cd_{xs}	**0.6**	**0.6**		0.1	0.3	**0.6**	**0.4**	**-0.4**	**0.5**	**-0.3**
Sterols	0.2	**0.4**	0.1		0.3	0.4	0.1	**-0.3**	**-0.4**	**-0.3**
GDGTs	0.3	**0.6**	0.3	0.2		0.3	**0.6**	**-0.4**	0.4	-0.2
C_{27} trisnorhopane	0.2	**0.5**	**0.6**	0.3	0.2		**0.5**	-0.3	0.4	**-0.4**
C_{31} hopanol	**0.5**	0.5	**0.5**	0.2	**0.6**	**0.5**		**-0.4**	0.4	-0.3
C_{32} hopanol	-0.3	**-0.5**	**-0.4**	-0.3	-0.4	-0.3	**-0.4**		-0.4	**0.3**
MAGEs	**0.6**	0.4	**0.5**	**-0.4**	0.4	0.4	0.4	-0.4		-0.2
PDO index	**-0.3**	-0.3	**-0.3**	**-0.3**	**-0.2**	**-0.4**	-0.2	**0.4**	**-0.2**	

1

2

Table 3. Molecules identified in m/z 191 mass chromatogram of aliphatic hydrocarbon and alcohol fractions from shelf sediments off Concepción (36ºS).

Hopanoid hydrocarbons

ID	Molecule	Number of carbon atoms	Molecular weight
1	17α-22,29,30-trinorhopane	27	370
2	22,29,30-trinor-17(21)-ene	27	368
3	17β-22,29,30-trinorhopane	27	370
4	17α,21α-30-norhopane	29	398
5	17β,21β-norhopene	27	368
6	17β,21β-hopane	30	412
7	Neohop-13(18)-ene	30	410
8	17α,21β-hopene	30	410
9	Hop-22(29)-ene	30	410
10	17α,21β-homohopane (R)	31	426
11	Diploptene	30	410
12	17α,21β-bishomohopane (R)	32	440
13	17β,21β-homohopane	31	426
$14_{S/R}$	17α,21β-trishomohopane (S-R)	33	454
$15_{S/R}$	17α,21β-tetrahomohopane (S-R)	34	468
$16_{S/R}$	17α,21β-pentakishomohopane (S-R)	35	482

Hopanols

ID	Molecule	Number of carbon atoms	Molecular weight
17	17β,21β-hopanol	30	500
18	17β,21β-homohopanol	31	514
19	17β,21β-bishomohopanol	32	528
20	17β,21β-trishomohopanol	33	542

3

4

5

6

7